*Geochemistry International, Vol. 40, No. 12, 2002, pp. 1139–1145. Translated from Geokhimiya, No. 12, 2002, pp. 1264–1270.*


# The Kaidun Meteorite: An Enstatite Aggregate with Sulfide–Oxide Inclusions

**A. V. Ivanov*, G. Kurat**, F. Brandstaetter**, N. N. Kononkova*, and L. F. Migdisova***

** Vernadsky Institute of Geochemistry and Analytical Chemistry, Russian Academy of Sciences, ul. Kosygina 19, Moscow, 119991 Russia*

*e-mail: andrei_ivanov@geokhi.ru*

*** Naturhistorisches Museum, A-1014 Vienna, Austria*

Received May 11, 2001

**Abstract**—An aggregate (approximately 0.5 mm across) examined in the Kaidun meteorite is dominated by prismatic crystals of enstatite ($Fs_{0.3–2.4}$, FeO/MnO = 1.9–13.6, up to 50 μm long) and contains rare grains of forsterite ($Fa_{0.5–0.6}$, FeO/MnO = 2.4–5.7), which are usually included in enstatite crystals. The interstitial space is filled with calcite a hydrated phase of variable composition. The hydrated phase contains small (<7 μm) inclusions of sulfide–oxide composition, whose cores consist mostly of Ti and Cr oxides and the rims of Mn and Fe sulfides. The composition and morphology of the enstatite and forsterite suggest that this aggregate is an agglomerate of nebular condensates that was not remelted. The oxide cores of the sulfide–oxide objects are early condensates of the nebula. The sulfide rims were produced during aqueous alterations in the parent body.

## INTRODUCTION

The heterogeneous breccia of Kaidun is characterized by the extreme diversity of its components. Along with fragments of the material of chondrites of various groups and classes and different achondrites, it contains aggregates that consist mostly of pure enstatite and have variable textures and associations of minor and accessory mineral phases [1, 2]. This paper is devoted to one of these aggregates, #d2-C, which exhibits no traces of melting of its material.

## METHODS

A polished thin section of the aggregate was studied by the conventional techniques of optical and scanning electron microscopy (on a Jeol JSM-6400 equipped with a Kevex energy-dispersion system). The chemical composition of phases was analyzed on ARL-SEMQ and Camebax-Microbeam X-ray probes. Most analyses were conducted at a current of 30 nA and an accelerating voltage of 15 kV. When the phases analyzed were expected to evaporate under the beam in standard mode, the analyses were carried out in the raster-scanning mode over an area with a sweep of 2 μm. The standards were natural minerals and synthetic compounds. The composition of the smallest objects, which could not be analyzed by EMPA techniques, was determined with an EDS detector. The analytical results were treated according to the ZAF and PAP correction procedures.

## TEXTURE AND MINERALOGY OF THE AGGREGATE

The aggregate is equant in shape with a visible cross-section of approximately 0.5 mm (Fig. 1). The boundary between the aggregate and the carbonaceous matrix is sharp, without any traces of interaction between the materials of the aggregate and matrix.

The aggregate is dominated by enstatite, the minor phases are forsterite, calcite, and a hydrated phase of complex composition, and the accessories are Ti and Cr oxides and sulfides (mostly of Mn).

Enstatite occurs in the form of euhedral prismatic crystals up to 50 μm long, which often compose aggregates, sometimes radiating (Fig. 2). The marginal parts of the crystals are occasionally corroded, the thickness of the altered zone is no more than 4 μm. Forsterite occurs in subordinate amounts and is usually included in enstatite crystals. Interstices between crystals are filled with the hydrated phase of complex composition and calcite. The interstitial phases usually do not form composite aggregates and intergrowths but occupy spatially separated areas.

A distinctive feature of the aggregate is the occurrence of numerous small (no larger than 7 μm) inclusions of Fe, Mn, Ti, and Cr sulfides and oxides in the interstitial hydrated phase (Fig. 3). The inclusions are often rounded in the thin-section plane, and their cores consist mainly of oxides, and their rims are dominated by sulfides. As is demonstrated by maps showing the distribution of elements (Fig. 4), Ti is concentrated in the central, "oxide" portions of these objects, whereas Cr is present also in the "sulfide" parts. Conceivably,

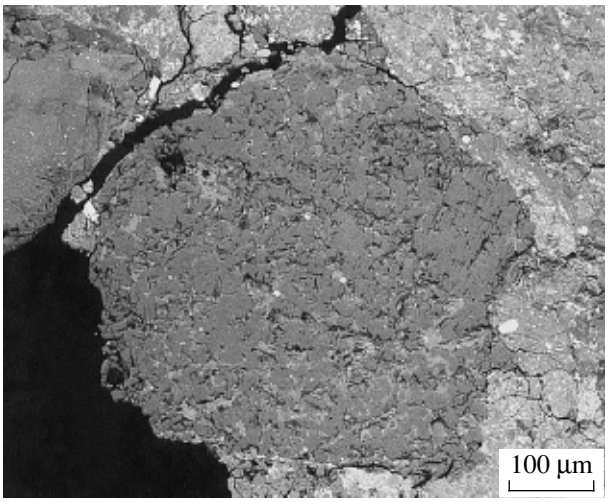


**Fig. 1.** Back-scattered electron image of aggregate Kaidun #d2-C surrounded by a carbonaceous matrix. Dark gray is enstatite, pale gray is calcite and the hydrated phase, and bright specks are sulfide–oxide objects. The scale bar is 100 μm.

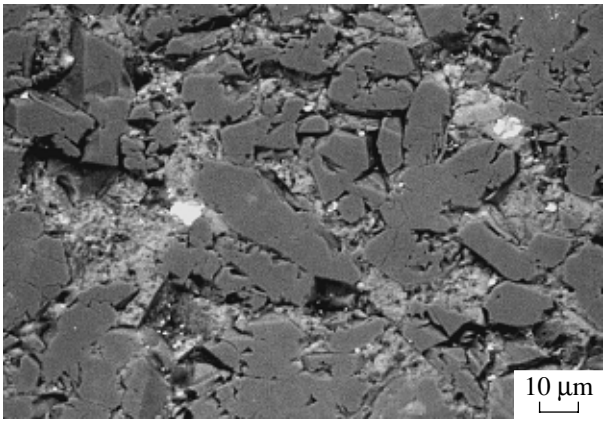


**Fig. 2.** Back-scattered electron image of a part of aggregate Kaidun #d2-C. The right-hand part of the image shows a druse-like aggregate of enstatite crystals. The interstitial hydrated phase contains two large sulfide–oxide inclusions. The scale bar is 10 μm.

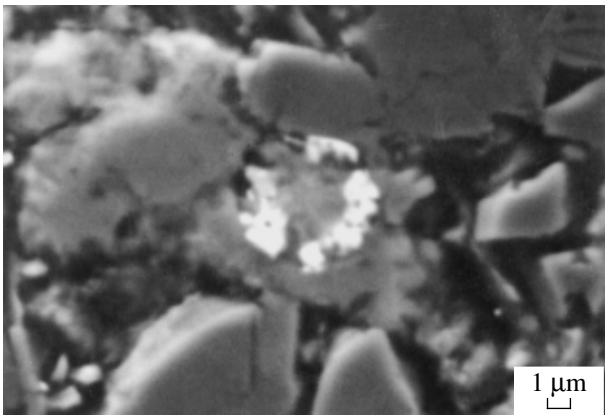


**Fig. 3.** Back-scattered electron image showing details of the inner structure of a large zoned sulfide–oxide inclusion. The pale gray oxide core is surrounded by a lighter discontinuous sulfide ring. The scale bar is 1 μm.

concentric inner structures of this type are characteristic of all of these inclusions but, of course, can be discerned only in certain cross sections. The hydrated phase also includes small patches enriched in Ti and/or Cr but devoid of Mn and S.

The hydrated phase was determined to contain small (~1–2 μm) $Al_2O_3$ grains. It should be mentioned that no $Al_2O_3$ was utilized as the polishing agent during the preparation of the thin section. However, we cannot fully rule out the possibility of contamination with this compound, which is widely used in thin-section preparation. Because of this, this phase will be rejected from the discussion.

## MINERAL CHEMISTRY

Enstatite, the dominant phase of the aggregate, shows (Table 1) significant variations in the concentrations of FeO ($Fs_{0.31–2.41}$), $Al_2O_3$, and MnO, as well as in the FeO/MnO ratio (1.93–13.56).

The composition of rare forsterite grains (Table 1) varies very little ($Fa_{0.49–0.59}$, FeO/MnO = 2.44–5.70).

The hydrated phase is characterized (Table 1) by low analytical totals (83.3–90.7 wt %) and fairly broad variations in the concentrations of most components, particularly silica and alumina. It is pertinent to note the strong negative correlations of $SiO_2$ with $Al_2O_3$ and $SiO_2$ with Cl and the positive correlations of $Al_2O_3$ with Cl and $TiO_2$ with $Cr_2O_3$ (Table 2).

The calcite contains 1.2 wt % MgO, 1.1 wt % MnO, and 0.44 wt % FeO on average.

The chemical composition of the small inclusions in the hydrated phase is listed in Table 3. The inclusions demonstrate strong positive correlations between Mn and S (Table 2), while the correlations of these two elements with other sulfide-forming elements (Mg and Ti) are strongly negative. The raw compositions yielded by analyses were recalculated to a two-component system. The proportions of the sulfide and oxide phases were determined based on the sulfur concentrations. The succession of ascribing elements to the sulfide phase in obtaining a stoichiometric MeS composition was based on the distribution character of elements in alabandite, the obvious main end member of sulfides in the objects. The recalculation results are summarized in Table 3, parts 2 and 3.

## GENESIS OF THE AGGREGATE

The broad variations in the chemistry of enstatite, the dominant phase of the aggregate, suggest that the latter was not remelted after its origin, because otherwise it would be logical to expect that the compositions of the minerals should be homogenized. The occurrence of radiation aggregates of enstatite crystals in this object is also consistent with this concept.

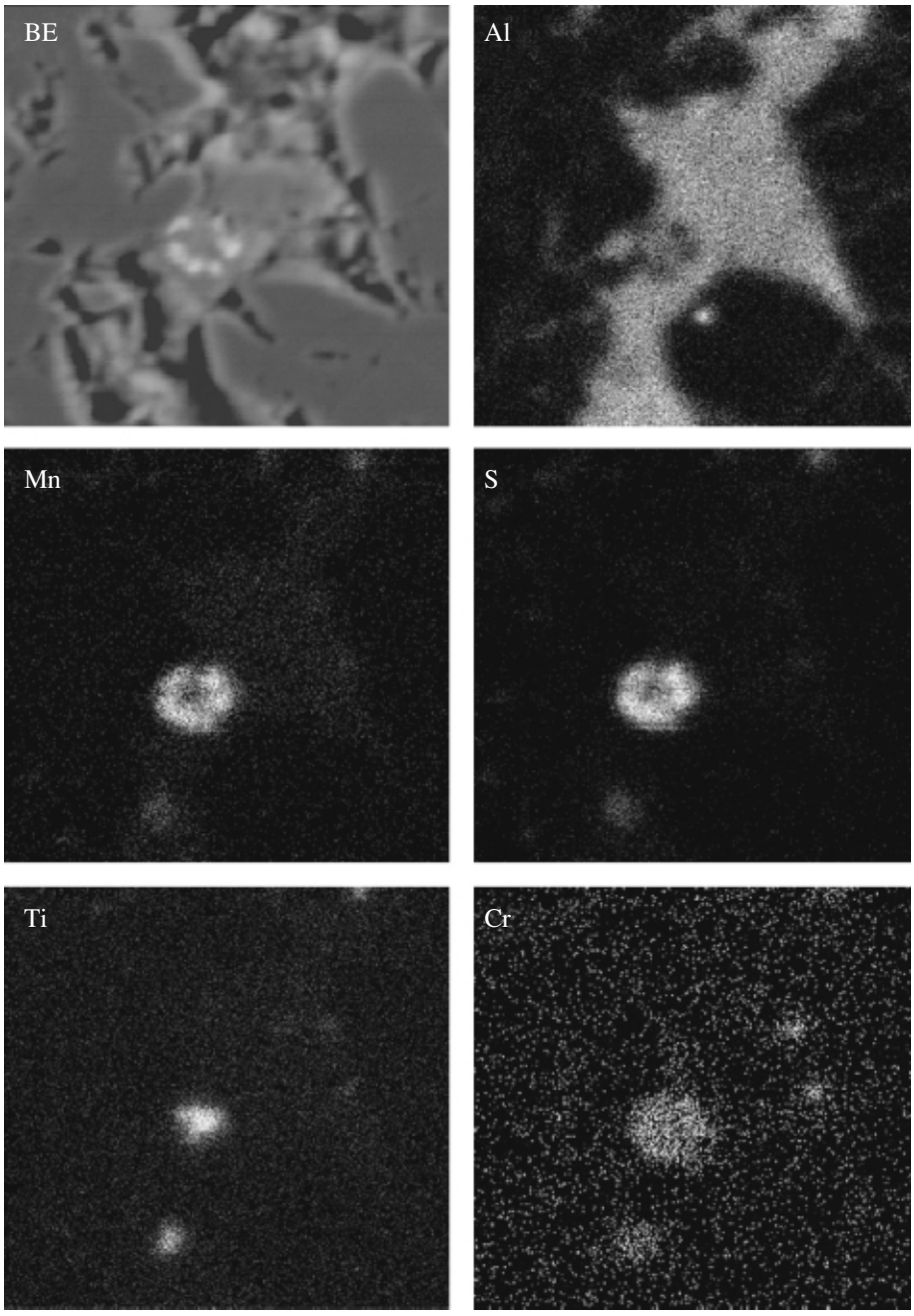


**Fig. 4.** Compositional maps of the distribution of some elements over an area with the sulfide–oxide inclusion shown in Fig. 3. BE is the back-scattered electron image, the others are images in the characteristic $k_\alpha$ radiation of Al, Mn, S, Ti, and Cr.

The compositions of the enstatite and forsterite are characterized by very low FeO/MnO ratios compared with those typical of chondrites (20–50, [3]). Such low-iron and manganese-enriched silicates (LIME) were earlier found in the porous particles of interplanetary dust, in the matrix of some unequilibrated chondrites, and in micrometeorites [3, 4]. They were also detected in the form of a CI clast in the Kaidun meteorite [5]. The origin of LIME is explained [3] by their condensation from a cooling gas of solar composition. Manganese, an element unstable in the metallic phase when occurring in the solar nebula, should have condensed as $Mn_2SiO_4$, in the form of a solid solution in forsterite.

It follows that aggregate #d2-C may be an agglomerate of the solar-nebula condensate that has not been remelted.

At the same time, the composition of the interstitial phase does not provide any grounds to relate its genesis to the condensation of the material from the nebula. The low analytical totals of the hydrated phase unambigu-

**Table 1.** Chemical composition (averages and variations, wt %) of silicate phases in aggregate Kaidun #d2-C

| Mineral | $SiO_2$ | $TiO_2$ | $Al_2O_3$ | $Cr_2O_3$ | FeO | MnO |
|---|---|---|---|---|---|---|
| Enstatite, $n$ = 26 | 60.2 | – | 0.30 | – | 0.62 | 0.10 |
| | 58.2–61.2 | <0.03–0.11 | 0.03–1.19 | <0.03–0.11 | 0.18–1.43 | 0.03–0.24 |
| Forsterite, $n$ = 7 | 43.2 | – | – | – | 0.44 | 0.13 |
| | 42.2–43.6 | <0.03 | <0.03–0.04 | <0.03–0.04 | 0.37–0.57 | 0.09–0.18 |
| Hydrated phase, $n$ = 14 | 28.4 | 0.55 | 15.1 | 0.16 | 19.9 | 0.84 |
| | 20.7–37.0 | 0.32–1.22 | 11.3–17.9 | 0.03–0.46 | 18.1–22.5 | 0.70–1.10 |
| Mineral | MgO | CaO | $Na_2O$ | Total | FeO/MnO | Fe/(Fe + Mg) at |
| Enstatite, $n$ = 26 | 39.0 | 0.19 | – | 100.41 | 6.37 | 0.92 |
| | 37.9–40.0 | 0.10–0.28 | <0.03–0.08 | 98.37–102.13 | 1.93–13.56 | 0.30–2.07 |
| Forsterite, $n$ = 7 | 55.4 | 0.06 | – | 99.23 | 3.49 | 0.44 |
| | 54.5–56.4 | 0.04–0.11 | <0.03 | 98.00–100.63 | 2.44–5.70 | 0.37–0.58 |
| Hydrated phase, $n$ = 14 | 19.9 | 0.43 | 0.35 | 86.83* | – | – |
| | 17.1–21.0 | 0.27–0.87 | 0.18–0.52 | 83.27–90.70 | – | – |

* Including (average/variations) $K_2O$ (0.42/0.30–0.66), S (0.48/0.25–0.78), and Cl (0.30/0.04–0.54).

**Table 2.** Correlation coefficients $r$ of some components in the hydrated phase and sulfide–oxide objects in aggregate Kaidun #d2-C

| Hydrated phase, $n$ = 14 | | | | Sulfide–oxide objects, $n$ = 8 | | | |
|---|---|---|---|---|---|---|---|
| Elements | $r$ | Elements | $r$ | Elements | $r$ | Elements | $r$ |
| Al–Cl | +0.90* | Si–Al | −0.97* | Mn–S | +0.97* | Mg–S | −0.96* |
| Ti–Cr | +0.82* | Si–Cl | −0.89* | | | Ti–Mn | −0.94* |
| | | | | | | Ti–S | −0.92* |
| Si–K | +0.66** | Al–K | −0.59** | Fe–Ti | +0.73** | Fe–Mn | −0.78** |
| Fe–S | +0.55** | | | | | Fe–S | −0.74** |
| Cl–S | +0.54** | | | | | | |

Note: One and two asterisks denote values significant at, respectively, 99 and 95% confidence levels for the respective samplings.

ously suggest that the phase contains water and, correspondingly, was produced under the effect of aqueous alterations. The process of aqueous alterations could occur both in the preaccretionary stage in the nebula (see, for example, [6]) and in the parent body (see, for example [7]). We identified both processes in the material of the Kaidun meteorite [8], and it was demonstrated that the products of the preaccretionary aqueous alterations of the nickel-iron are characterized by a fairly little varying equilibrium composition at the virtual absence of Cl, while the alteration products in the parent body, conversely, show a wide spread in the aqueous alteration products and notable Cl concentrations.

The chemistry of the hydrated phase in the aggregate and broad variations in its composition suggest that the alteration process was obviously unequilibrated and, perhaps, proceeded at a relatively low temperature. This character of the process evidently corresponds to aqueous alterations in the parent body. The presence of notable Cl amounts in the hydrated phase is compatible with the process of aqueous alterations in the parent body.

Calcite in the Kaidun meteorite was previously found in fragments of various lithological types [9, 10]. The origin of this mineral is though to have been related to aqueous alterations in the parent body, and it was demonstrated that these processes in the Kaidun meteorite took place early in the stage of the origin of the material [10]. Hence, the occurrence of calcite is fully consistent with the crystallization of the interstitial

**Table 3.** Chemical composition (wt %, normalized to 100%) of small sulfide–oxide objects in aggregate Kaidun #d2-C

Part 1. Raw analysis (oxide mode)

| Number and location | Si | Ti | Al | Cr | Fe | Mn | Mg | Ca | Na | K | Ni | S | $O_{calcd}$ |
|---|---|---|---|---|---|---|---|---|---|---|---|---|---|
| 1, Rim | 2.18 | 0.25 | 0.48 | 1.13 | 13.02 | 15.59 | 3.03 | 0.75 | 0.36 | <0.1 | 0.68 | 19.23 | 43.27 |
| 1, Core | 7.74 | 8.85 | 2.83 | 2.35 | 15.06 | 5.69 | 5.06 | 0.72 | 0.89 | 0.13 | 0.25 | 8.78 | 41.65 |
| 4, Rim | 2.06 | 1.66 | 0.66 | 1.75 | 13.43 | 15.09 | 2.36 | 2.47 | 0.41 | 0.13 | 0.52 | 17.43 | 42.04 |
| 4, Core | 12.35 | 6.76 | 4.32 | 3.25 | 15.90 | 2.40 | 8.29 | 0.99 | 1.19 | 0.38 | 0.34 | 3.19 | 40.64 |
| 5, Rim | 3.14 | 0.70 | 1.29 | 1.36 | 15.05 | 14.28 | 2.86 | 0.45 | 0.39 | 0.07 | 1.53 | 16.81 | 42.08 |
| 5, Core | 10.15 | 9.36 | 3.88 | 1.54 | 17.78 | 2.91 | 5.66 | 0.56 | 0.82 | 0.33 | 0.25 | 5.79 | 40.96 |
| 2 | 0.24 | 0.17 | <0.1 | 1.60 | 13.59 | 14.74 | 1.79 | 1.40 | 0.21 | <0.1 | 0.30 | 21.91 | 44.02 |
| 3 | 1.77 | 0.26 | 0.50 | 1.83 | 14.86 | 13.11 | 2.45 | 0.95 | 0.39 | 0.17 | 0.77 | 19.63 | 43.32 |

Part 2. Composition of sulfides

| Number and location | Percentage of sulfides in the overall composition | S | Mn | Fe | Mg | Ca | Cr | Ti | Ni | $MnS_{mol}$ | $FeS_{mol}$ | $MgS_{mol}$ |
|---|---|---|---|---|---|---|---|---|---|---|---|---|
| 1, Rim | 78.5 | 39.4 | 31.9 | 26.6 | 2.1 | – | – | – | – | 50.8 | 41.7 | 7.5 |
| 1, Core | 29.2 | 36.6 | 23.7 | 39.7 | – | – | – | – | – | 37.8 | 62.2 | – |
| 4, Rim | 71.5 | 37.4 | 32.4 | 28.8 | 1.5 | – | – | – | – | 50.6 | 44.2 | 5.2 |
| 4, Core | 9.3 | 36.6 | 27.5 | 35.8 | – | – | – | – | – | 43.9 | 56.1 | – |
| 5, Rim | 69.0 | 36.7 | 31.2 | 32.2 | – | – | – | – | – | 49.6 | 50.4 | – |
| 5, Core | 18.3 | 36.6 | 18.4 | 45.0 | – | – | – | – | – | 29.4 | 70.6 | – |
| 2 | 98.6 | 39.5 | 26.5 | 24.5 | 3.2 | 2.5 | 2.9 | 0.3 | 0.5 | 45.8 | 41.6 | 12.6 |
| 3 | 82.8 | 39.0 | 26.0 | 29.5 | 4.9 | 0.6 | – | – | – | 39.4 | 44.0 | 16.6 |

Part 3. Composition of oxides

| Number and location | Percentage of oxides in the overall composition | $SiO_2$ | $TiO_2$ | $Al_2O_3$ | $Cr_2O_3$ | FeO | MgO | CaO | $Na_2O$ | $K_2O$ | NiO |
|---|---|---|---|---|---|---|---|---|---|---|---|
| 1, Rim | 21.5 | 34.9 | 3.0 | 6.7 | 12.4 | – | 24.9 | 7.9 | 3.6 | 0.1 | 6.4 |
| 1, Core | 70.8 | 28.4 | 25.4 | 9.2 | 5.9 | 12.2 | 14.4 | 1.7 | 2.0 | 0.3 | 0.5 |
| 4, Rim | 28.5 | 23.8 | 14.9 | 6.6 | 13.7 | – | 15.0 | 18.5 | 3.0 | 0.8 | 3.6 |
| 4, Core | 90.7 | 31.2 | 13.3 | 9.6 | 5.6 | 19.4 | 16.2 | 1.6 | 1.9 | 0.5 | 0.5 |
| 5, Rim | 31.0 | 32.7 | 5.7 | 11.8 | 9.6 | 1.8 | 23.0 | 3.1 | 2.5 | 0.5 | 9.4 |
| 5, Core | 81.7 | 30.8 | 22.1 | 10.4 | 3.2 | 16.5 | 13.3 | 1.1 | 1.6 | 0.6 | 0.4 |
| 2 | 1.4* | | | | | | | | | | |
| 3 | 17.2 | 36.2 | 4.1 | 9.0 | 25.6 | – | – | 8.8 | 5.1 | 1.8 | 9.4 |

Note: Dashes mean the absence of the component in the phase.

* Composition was not calculated because of the very low overall concentration of oxides.

phases of the aggregate as a consequence of the aqueous alteration of material in the parent body.

The notable Cl concentrations in the hydrated phase of the aggregate seem to have been introduced in the process of aqueous alterations, and the correlations between components in this phase (Table 3) suggest that the aqueous alteration process was accompanied by the introduction of Al, Fe, and S and the removal of Si and K. However, currently available data are still obviously insufficient for any definite conclusions concerning the composition of the primary phase.

The small sulfide–oxide inclusions in the hydrated phase are concentrically zoned (Fig. 4): Mn-rich sulfide (alabandite) surrounds a core enriched in Cr and Ti sulfides, with the Ti oxide occurring at the center of the oxide core. This inner texture obviously suggests the origin of the objects in a number of stages and definitely indicates that oxides, first of all, Ti oxide, were the first to form.

There are no reasons to believe that either Ti oxide or its other oxygen-bearing compounds were produced in the course of aqueous alterations (Ti is one of the least mobile elements in most geochemical processes). However, taking into account the aforementioned distinctive features of the aggregate, which suggest that enstatite, the dominant mineral of the aggregate, was produced by condensation, and the fact that the Ti minerals were among the earliest condensation products in the cooling solar nebula, it is realistic to hypothesize that Ti- and Cr-rich phases are also of condensation genesis.

The small sulfide–oxide objects seem to have been formed in compliance with the following scenario. According to currently adopted models for the equilibrium condensation of a gas of solar composition under a pressure of $10^{-3}$ atm [11–13], Ti should have condensed in the form of perovskite $CaTiO_3$ early during this process, starting from the temperature of 1650 K. Later, perovskite was transformed to Ti oxide by a gas–solid reaction in the nebula. Calculations of the gas composition under somewhat different conditions indicate that $TiO_2$ should condense at a temperature of 1616 K [14]. Chromium could condense in the form of a solid solution in metallic iron starting from a temperature of approximately 1470 K [15]. The oxidation of the metallic phase and the transition of Cr to the oxide mode could take place during a change in the redox conditions in the nebula. The Ti- and Cr-rich nebular condensate was captured by a precursor of the hydrated phase. These objects in the aggregate can, perhaps, be regarded as an analogue of the oxide inclusions (MgO, $TiO_2$, CaO, and $Al_2O_3$) that were found in Ca- and Al-rich inclusions of carbonaceous chondrites [14]. It should be mentioned, however, that the oxide inclusions in the CAI of carbonaceous chondrites are 50–200 nm in size [14], whereas the sizes of the Ti oxide core in inclusions in our sample of the Kaidun meteorite are as large as 2 μm.

It seems that two distinct mechanisms that resulted in the development of the alabandite rims of the Ti and Cr oxides are possible. One of them is related to MnS condensation from the nebula starting at a temperature of approximately 1200 K. However, the condensation of Ti- and Cr-bearing components and Mn sulfide was separated by a significant temperature interval in which the main silicate minerals were condensed. It is hard to believe that the early condensates were therewith preserved in the nebula in a separated state.

An alternative process is the origin of alabandite in the parent body under the effect of aqueous alterations. This process was coupled with the mobilization of Mn from the hydrated phase and the concentration of this element around Ti- and Cr-rich inclusions. Sulfur, which was introduced during the aqueous alterations, reacted with manganese. It should be noted that low-temperature hydrothermal genesis is very typical of alabandite under terrestrial conditions [16].

## ACKNOWLEDGMENTS

This study was supported by the Russian Foundation for Basic Research, project nos. 97-05-64378 and 01-05-64239, the Austrian Academy of Sciences, and the FWF (Austria).

## REFERENCES

1. Kurat, G., Zinner, E., Brandstaetter, F., and Ivanov, A., The Kaidun Meteorite: An Enstatite Clast with Niningerite and Heideite as Trace Element Carriers, *Meteorit. Planet. Sci.*, 1997, vol. 32, suppl., pp. A76–A77.
2. Ivanov, A., Brandstaetter, F., Kurat, G., *et al.*, The Kaidun Meteorite: An Unmelted Enstatite Aggregate, *Meteorit. Planet. Sci.*, 1998, vol. 33, suppl., pp. A75–A76.
3. Klock, W., Thomas, K.L., McKay, D.S., and Palme, H., Unusual Olivine and Pyroxene Composition in Interplanetary Dust and Unequilibrated Ordinary Chondrites, *Nature* (London), 1989, vol. 339, pp. 126–128.
4. Presper, T., Kurat, G., and Maurette, M., Preliminary Report on the Composition of Anhydrous Primary Mineral Phases in Micrometeorites from Cap Prudhomme, Antarctica, *Meteoritics*, 1992, vol. 27, p. 278.
5. Brandstaetter, F., Kurat, G., and Ivanov, A.V., Isolated Minerals in Kaidun II (CI), *Meteoritics*, 1992, vol. 27, p. 206.
6. Metzler, K., Bischoff, A., and Stoffler, D., Accretional Dust Mantles in CM Chondrites: Evidence for Solar Nebula Processes, *Geochim. Cosmochim. Acta*, 1992, vol. 56, pp. 2873–2897.
7. Zolensky, M. and McSween, H.Y., Aqueous Alteration, in *Meteoritics and the Early Solar System*, Kerridge, J.F. and Matthews, M.S., Eds., 1988, Univ. of Arizona Press, pp. 114–143.
8. Ivanov, A.V., Kurat, G., Migdisova, L.F., *et al.*, The Kaidun Meteorite: Pre- and Post-Accretional Aqueous Alterations of Metal in a Carbonaceous Chondrite Fragment, *Geokhimiya*, 1998, no. 2, pp. 131–136.
9. Weisberg, M.K., Prinz, M., Zolensky, M.E., and Ivanov, A.V., Carbonates in the Kaidun Meteorite, *Meteoritics*, 1994, vol. 29, pp. 549–550.
10. Hutcheon, I.D., Weisberg, M.K., Phinney, D.L., *et al.*, Radiogenic $^{53}Cr$ in Kaidun Carbonates: Evidence for Very Early Aqueous Activity, *Lunar Planet. Sci. XXX*, 1999, p. 1722.

11. Grossman, L., Condensation in the Primitive Solar Nebula, *Geochim. Cosmochim. Acta*, 1972, vol. 36, pp. 597–619.

12. Wood, J. and Hashimoto, A., Mineral Equilibrium in the Solar Nebula, *Geochim. Cosmochim. Acta*, 1993, vol. 57, pp. 2377–2385.

13. Shapkin, A.I. and Sidorov, Yu.I., *P–T* Dependence of the Density of Nebular Condensate, *Geokhimiya*, 1997, no. 12, pp. 1196–1207.

14. Greshake, A., Bischff, A., Putnis, A., and Palme, H., Corundum, Rutile, Periclase, and CaO in Ca–Al-Rich Inclusions from Carbonaceous Chondrites, *Science*, 1996, vol. 272, pp. 1316–1318.

15. Grossman, L. and Olsen, E., Origin of the High-Temperature Fraction of C2 Chondrites, *Geochim. Cosmochim. Acta*, 1974, vol. 38, pp. 173–187.

16. *Mineraly. Spravochnik* (Minerals. Reference Book), Chukhrov, F.V., Ed., Moscow: Akad. Nauk SSSR, 1960, vol. 1, pp. 192–194.